ACS APPLIED MATERIALS & INTERFACES

Letter

www.acsami.org

$CoSe_2$ Nanowires Array as a 3D Electrode for Highly Efficient Electrochemical Hydrogen Evolution

Qian Liu,[†] Jinle Shi,[‡] Jianming Hu,[‡] Abdullah M. Asiri,[§] Yonglan Luo,*[,†] and Xuping Sun*[,†]

[†]Chemical Synthesis and Pollution Control Key Laboratory of Sichuan Province, College of Chemistry and Chemical Engineering, China West Normal University, Nanchong, 637002 Sichuan, China

[‡]Optical Engineering Key Laboratory of Chongqing Municipal Education Commission, College of Physics and Information Technology, Chongqing Normal University, Chongqing 40047, China

[§]Chemistry Department, Faculty of Science, King Abdulaziz University, Jeddah 21589, Saudi Arabia

Supporting Information

ABSTRACT: In this Letter, we describe the development of a $CoSe_2$ nanowires array on carbon cloth ($CoSe_2$ NW/CC) through a facile two-step hydrothermal preparative strategy. As a novel 3D nanoarray electrode for electrochemical hydrogen evolution, $CoSe_2$ NW/CC exhibits excellent catalytic activity and durability in acidic media. It needs overpotentials of 130 and 164 mV to approach 10 and 100 mA cm^{-2}, respectively, and its activity is maintained for at least 48 h. This work would open up new avenues for the rational design of a variety of arrayed transition-metal chalcogenide cathodes for technological application toward large-scale hydrogen generation from water.

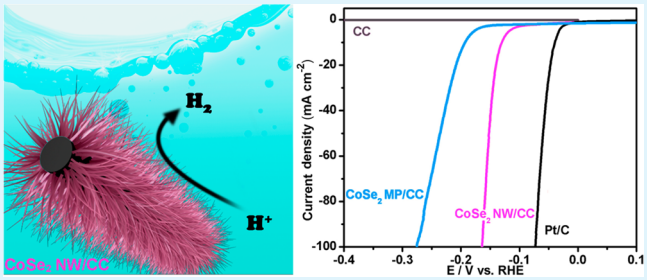

KEYWORDS: *$CoSe_2$ nanowires, array electrode, anion exchange reaction, hydrogen evolution, electrocatalysis*

Fossil fuels not only create pollution and a carbon footprint but also face a depletion issue. Hydrogen is a promising alternative and renewable energy source to replace fossil fuels in the future. Electrochemical water splitting offers a simple way to produce highly pure hydrogen. To make the whole process more energy efficient, an efficient hydrogen evolution reaction (HER) electrocatalyst is, however, needed to achieve high current at low overpotential.[1] Compared to traditional alkaline technologies, proton-exchange-membrane water electrolysis possesses several advantages of greater energy efficiency, higher production rates, and more compact design,[2] while the strongly acidic conditions involved require the use of acid-stable HER catalysts.[3] Platinum-group metals show the best catalytic activity, but the high cost and rareness of such catalysts impede their widespread use in the industry.[4] Although earth-abundant nickel-based transition-metal alloys are capable of efficiently catalyzing the HER in alkaline media, they suffer from poor stability in acidic solutions because of a corrosion issue.[5−7] As such, it is highly desired to develop and design highly active, acid-stable HER catalysts based on earth-abundant materials.

Cobalt has emerged as an interesting nonprecious metal with catalytic power toward hydrogen evolution, and recent years have witnessed the huge progress achieved in developing cobalt-based molecular complexes as HER catalysts.[8−10] Such homogeneous catalysts, however, usually suffer from a large overpotential and/or low stability,[10] and it is also highly challenging to graft them onto electrodes for practical application.[11] We and other researchers have recently proven that these problems can be overcome by using solid-state cobalt phosphide based heterogeneous catalysts.[12−14] Cobalt chalcogenides including CoS_2 and $CoSe_2$ are metal conductors,[15,16] offering them a unique advantage as electrocatalysts, and much recent efforts have been devoted to making crystalline CoS_2/$CoSe_2$ for catalysis of the HER in acidic media.[15,17−21] Kong et al. developed thin films of CoS_2 and $CoSe_2$ by thermal sulfidation/selenization of an e-beam-evaporated cobalt precursor on a glassy carbon substrate.[17] Faber et al. utilized the same strategy to prepare a CoS_2 thin film on a graphite support.[18] Further enhanced catalytic activity can be achieved by growing a CoS_2 microwires (MWs) and nanowires (NWs) film on a 2D substrate[15] or developing a $CoSe_2$ nanoparticles film on a 3D carbon fiber paper ($CoSe_2$ NP/CP).[19] Such a vapor-based high-temperature technique for catalyst preparation, however, requires a relatively high energy input and lacks compatibility with substrates, and it is thus likely not cost-effective for large-scale applications. Xu et al. reported a hydrothermal−solvothermal−annealing route to make Ni/NiO/$CoSe_2$ nanocomposites at lower temperatures, but this catalyst is unstable in acidic media.[20] More recently, Gao et al. developed a MoS_2/$CoSe_2$ hybrid HER electrocatalyst using a high-temperature hydrazine solvothermal method.[21]

Received: December 30, 2014
Accepted: February 13, 2015
Published: February 13, 2015

DOI: 10.1021/am509185x
ACS Appl. Mater. Interfaces 2015, 7, 3877−3881

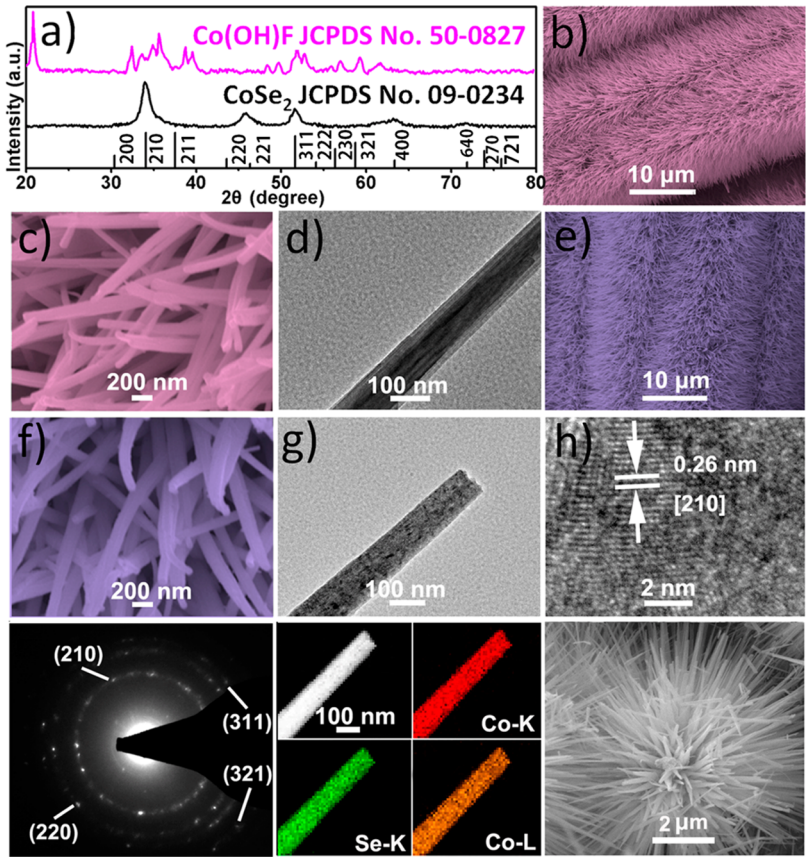

Figure 1. (a) XRD patterns of the precursor and selenized product scratched down from CC. (b and c) SEM images of Co(OH)F NW/CC. (d) TEM image of a Co(OH)F NW. (e and f) SEM images of $CoSe_2$ NW/CC. (g) TEM image of a $CoSe_2$ NW. (h) HRTEM image and (i) SAED pattern taken from a $CoSe_2$ NW. (j) STEM image and EDX elemental mapping of cobalt and selenium for a $CoSe_2$ NW. (k) SEM image of a $CoSe_2$ MP.

In this Letter, we report a facile two-step approach for the low-temperature hydrothermal fabrication of a $CoSe_2$ NWs array on carbon cloth ($CoSe_2$ NW/CC): hydrothermal growth of a Co(OH)F NW on CC[12] followed by hydrothermal conversion into a $CoSe_2$ NW through an anion-exchange reaction[22] [see the Supporting Information (SI) for preparation details]. When directly used as an integrated 3D array electrode for the HER in acidic media, the $CoSe_2$ NW/CC shows exceptionally high catalytic activity, superior to that reported for $CoSe_2$ NP/CP and films of CoS_2 MWs and CoS_2 NWs, with the need for overpotentials of 130 and 164 mV to achieve 10 and 100 mA cm^{-2}, respectively. This electrode is also excellent in durability, with its catalytic activity being maintained for at least 48 h. This development offers us a promising hydrogen evolution cathode for large-scale electrochemical water-splitting application.

Figure 1a presents the powder X-ray diffraction (XRD) patterns of the precursor and selenized product scratched down from CC. As observed, the precursor shows characteristic peaks of orthorhombic Co(OH)F (JCPDS 50-0827),[12] while the selenized product only exhibits diffraction peaks corresponding to cubic-phase $CoSe_2$ (JCPDS 09-0234),[16,23] suggesting the successful conversion of Co(OH)F into $CoSe_2$. Figure 1b shows the low-magnification scanning electron microscopy (SEM) image of Co(OH)F NW/CC, clearly indicating full coverage of CC by Co(OH)F NWs. The high-magnification SEM image (Figure 1c) shows that these NWs have diameters in the range of 90−160 nm and are a few micrometers in length. The transmission electron microscopy (TEM) image further reveals that such NWs have a smooth surface, as shown in Figure 1d. After hydrothermal selenization reaction, the resulting $CoSe_2$ product still retains 1D morphology and an integration feature (Figure 1e,f) but with a rough surface (Figure 1g). The high-resolution TEM (HRTEM) image taken from $CoSe_2$ NWs (Figure 1h) shows a lattice fringe with an interplane spacing of 0.26 nm corresponding to the (210) plane of $CoSe_2$. The corresponding selected-area electron diffraction (SAED) pattern (Figure 1i) reveals discrete spots indexed to the (210), (220), (311), and (321) planes of the cubic-phase $CoSe_2$.[16] Scanning TEM (STEM) image and energy-dispersive X-ray (EDX) elemental mapping images of cobalt and seleniun for $CoSe_2$ NWs further demonstrate the uniform distribution of both cobalt and selenium elements in the whole NW, as shown in Figure 1j. The same preparation without the involvement of CC leads to urchin-like microspheres (MPs) consisting of Co(OH)F NWs, and the following selenization gives $CoSe_2$ MPs with urchin-like morphology (Figure S1 in the SI and Figure 1k).

We investigated the HER activity of $CoSe_2$ NW/CC ($CoSe_2$ loading: ~1.3 mg cm^{-2}) as a 3D integrated electrode in 0.5 M H_2SO_4 at room temperature using a typical three-electrode setup. Commercial Pt/C (20 wt % Pt/XC-72) showing high HER activity with near-zero overpotential was chosen as a reference point. The HER activities for both bare CC and $CoSe_2$ MP/CC ($CoSe_2$ MP was immobilized on CC with the same loading using a Nafion solution) were also examined for

DOI: 10.1021/am509185x
ACS Appl. Mater. Interfaces 2015, 7, 3877−3881

comparison purposes. To reflect the intrinsic electrocatalytic activity of the catalysts, an *iR* correction was applied to all initial data for further analysis.[24] The measured polarization curves are shown in Figure 2a. Bare CC has poor HER activity. In

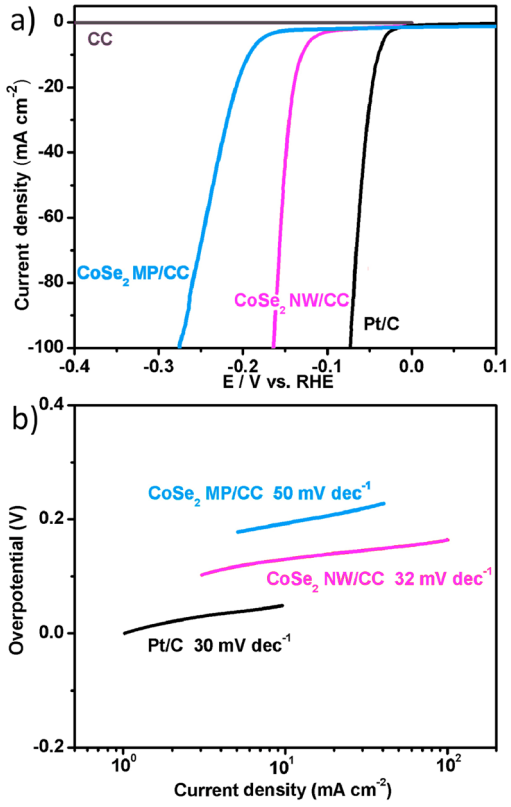

Figure 2. (a) Polarization curves for Pt/C, $CoSe_2$ NW/CC, $CoSe_2$ MP/CC, and CC. (b) Tafel plots for platinum/carbon, $CoSe_2$ NW/CC, and $CoSe_2$ MP/CC.

contrast, $CoSe_2$ MP/CC is highly active toward the HER with an onset overpotential of 149 mV, beyond which the cathodic current rises sharply under more negative potential. This electrode shows current densities of 10 and 100 mA cm^{-2} at overpotentials of 193 and 275 mV, respectively. However, $CoSe_2$ NW/CC exhibits a more positive overpotential of 85 mV for the HER with much larger cathodic current densities (10 and 100 mA cm^{-2} at 130 and 164 mV, respectively). These overpotentials are the lowest among all reported values for acid-stable cobalt chalcogenide HER catalysts except $MoS_2/CoSe_2$ (Table S1 in the SI).

The Tafel slope is an inherent property of electrocatalysts, and a small Tafel slope leads to a strongly enhanced HER rate at a moderate increase of overpotential.[25] According to the HER kinetic models, Tafel slopes of ~30, ~40, or ~120 mV dec^{-1} will be achieved if the Tafel, Heyrovsky, or Volmer step is the rate-determining step, respectively.[21] To gain further insight into the $CoSe_2$ NW/CC electrode, we investigated the Tafel plots for $CoSe_2$ NW/CC, $CoSe_2$ MP/CC, and Pt/C. The resulting Tafel slope of $CoSe_2$ NW/CC is 32 mV dec^{-1}, which is much lower than that of $CoSe_2$ MP/CC (50 mV dec^{-1}) and very close to the value of Pt/C (30 mV dec^{-1}). To the best of our knowledge, this value is the lowest for all recorded cobalt chalcogenide catalysts listed in Table S1 in the SI and other non-noble-metal HER catalysts in acidic media except FeP/CC (32 mV dec^{-1}).[26] The Tafel slope for $CoSe_2$ NW/CC suggests that the HER proceeds via a Volmer–Tafel mechanism, for which the Tafel step is the rate-determining step.[21] This performance of the $CoSe_2$ NW/CC electrode suggests that it may hold great promise for practical applications.

To assess the durability of the $CoSe_2$ NW/CC and $CoSe_2$ MP/CC electrodes in strongly acidic media, we conducted potential sweeps between +0.1 and −0.3 V versus RHE for 1000 cycles. After cycling, the $CoSe_2$ NW/CC electrode shows a polarization curve similar to that before testing, while $CoSe_2$ MP/CC exhibits distinct degradation of the activity, as shown in Figure 3a. We also performed electrolysis experiments on

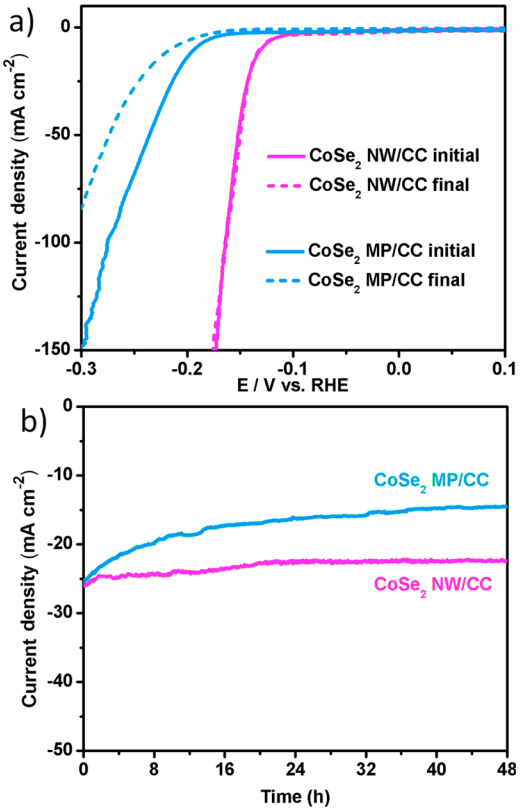

Figure 3. (a) Polarization curves for $CoSe_2$ NW/CC and $CoSe_2$ MP/CC in 0.5 M H_2SO_4 initially and after 1000 potential sweeps between +0.1 and −0.3 V vs RHE at a scan rate of 100 mV s^{-1}. (b) Time-dependent current density curves for $CoSe_2$ NW/CC and $CoSe_2$ MP/CC at fixed overpotential in 0.5 M H_2SO_4.

both electrodes. It is seen that $CoSe_2$ NW/CC retains its activity for at least 48 h at an overpotential of 143 mV, but a dramatic loss in the current density is observed for $CoSe_2$ MP/CC at an overpotential of 214 mV under the same timeframe (Figure 3b). Furthermore, after 2 h of continuous cyclic voltammetry, the SEM image (Figure S2a in the SI) of $CoSe_2$ NW/CC shows that it preserves its morphology, and the XRD pattern (Figure S2b in the SI) further reveals no change in the crystal structure of $CoSe_2$. These observations imply the superior stability of $CoSe_2$ NW/CC over $CoSe_2$ MP/CC in a long-term electrochemical process.

The excellent HER activity and durability for $CoSe_2$ NW/CC could be rationally explained as follows. (1) The nanoarray format allows for exposure of more active sites.[27] Furthermore, the 3D configuration of this electrode facilitates efficient diffusion of the electrolyte, and H_2 gas evolved. (2) The direct growth of $CoSe_2$ on CC offers intimate contact, good

DOI: 10.1021/am509185x
ACS Appl. Mater. Interfaces 2015, 7, 3877–3881

mechanical adhesion, and excellent electrical connection between them. (3) The absence of polymer binder for catalyst immobilization not only avoids the blocking of active sites and inhibition[28] but decreases the series resistance.[29] Electrochemical impedance spectroscopy measurements (Figure S3 in the SI) confirm that $CoSe_2$ NW/CC has much lower impedance and, hence, markedly faster HER kinetics than $CoSe_2$ MP/CC.[30]

Note that we have failed to obtain a CoS_2 NWs array through the same method using S power as the precursor. The SEM image indicates that CC was also fully covered by a NWs array after sulfidation reaction, as shown in Figure S4a in the SI. The EDX spectrum (Figure S4b in the SI) shows incomplete conversion of Co(OH)F, and the atomic ratio of the product for Co:S is 55:16. The corresponding XRD pattern for the product (Figure S4c in the SI) is unmatched with the standard XRD pattern of CoS_2. Although this array is also electroactive toward the HER, it displays 10 mA cm^{-2} at overpotential of 276 mV with inferior activity over $CoSe_2$ NW/CC, as shown in Figure S4d in the SI.

In conclusion, a $CoSe_2$ NWs array has been developed on carbon cloth via a two-step hydrothermal approach. This 3D architecture can be directly used as a nanoarray electrode for electrochemical hydrogen evolution in acidic solutions with high activity and durability. This study has opened new avenues to hydrothermally fabricating binder-free hydrogen-evolving cathodes based on transition-metal chalcogenides for applications toward large-scale hydrogen production from water.

■ ASSOCIATED CONTENT

Supporting Information

Experimental section, SEM images, XRD patterns, Table S1, Nyquist plots, EDX spectrum, and polarization curve. This material is available free of charge via the Internet at http://pubs.acs.org.

■ AUTHOR INFORMATION

Corresponding Authors

*E-mail: luoylcwnu@hotmail.com.
*E-mail: sunxp@cwnu.edu.cn.

Notes

The authors declare no competing financial interest.

■ REFERENCES

(1) Walter, M. G.; Warren, E. L.; McKone, J. R.; Boettcher, S. W.; Mi, Q.; Santori, E. A.; Lewis, N. S. Solar Water Splitting Cells. *Chem. Rev.* **2010**, *110*, 6446−6473.

(2) Marshall, A.; Børresen, B.; Hagen, G.; Tsypkin, M.; Tunold, R. Hydrogen Production by Advanced Proton Exchange Membrane (PEM) Water Electrolysers—Reduced Energy Consumption by Improved Electrocatalysis. *Energy* **2007**, *32*, 431−436.

(3) Goff, A. L.; Artero, V.; Jousselme, B.; Tran, P. D.; Guillet, N.; Métayé, R.; Fihri, A.; Palacin, S.; Fontecave, M. From Hydrogenases to Noble Metal-Free Catalytic Nanomaterials for H_2 Production and Uptake. *Science* **2009**, *326*, 1384−1387.

(4) Greeley, J.; Jaramillo, T. F.; Bonde, J.; Chorkendorff, I.; Norskov, J. K. Computational High-throughput Screening of Electrocatalytic Materials for Hydrogen Evolution. *Nat. Mater.* **2006**, *5*, 909−913.

(5) Raj, I. A.; Vasu, K. I. Transition Metal-based Hydrogen Electrodes in Alkaline Solution-electrocatalysis on Nickel Based Binary Alloy Coatings. *J. Appl. Electrochem.* **1990**, *20*, 32−38.

(6) Gao, M.; Lin, Z.; Zhuang, T.; Jiang, J.; Xu, Y.; Zheng, Y.; Yu, S. Mixed-Solution Synthesis of Sea Urchin-like NiSe Nanofiber Assemblies as Economical Pt-free Catalysts for Electrochemical H_2 Production. *J. Mater. Chem.* **2012**, *22*, 13662−13668.

(7) Gao, M.; Xu, Y.; Jiang, J.; Yu, S. Nanostructured Metal Chalcogenides: Synthesis, Modification, and Applications in Energy Conversion and Storage Devices. *Chem. Soc. Rev.* **2013**, *42*, 2986−3017.

(8) Losse, S.; Vos, J. G.; Rau, S. Catalytic Hydrogen Production at Cobalt Centres. *Coord. Chem. Rev.* **2010**, *254*, 2492−2504.

(9) Artero, V.; Chavarot-Kerlidou, M.; Fontecave, M. Splitting Water with Cobalt. *Angew. Chem., Int. Ed.* **2011**, *50*, 7238−7266.

(10) Artero, V.; Fontecave, M. Solar Fuels Generation and Molecular Systems: Is It Homogeneous or Heterogeneous Catalysis? *Chem. Soc. Rev.* **2013**, *42*, 2338−2356.

(11) Andreiadis, E. S.; Jacques, P.-A.; Tran, P. D.; Leyris, A.; Chavarot-Kerlidou, M.; Jousselme, B.; Matheron, M.; Pécaut, J.; Palacin, S.; Fontecave, M.; Artero, V. Molecular Engineering of a Cobalt-Based Electrocatalytic Nanomaterial for H_2 Evolution under Fully Aqueous Conditions. *Nat. Chem.* **2013**, *5*, 48−53.

(12) Tian, J.; Liu, Q.; Asiri, A. M.; Sun, X. Self-Supported Nanoporous Cobalt Phosphide Nanowire Arrays: An Efficient 3D Hydrogen-Evolving Cathode over the Wide Range of pH 0−14. *J. Am. Chem. Soc.* **2014**, *136*, 7587−7590.

(13) Pu, Z.; Liu, Q.; Jiang, P.; Asiri, A. M.; Obaid, A. Y.; Sun, X. CoP Nanosheet Arrays Supported on a Ti Plate: An Efficient Cathode for Electrochemical Hydrogen Evolution. *Chem. Mater.* **2014**, *26*, 4326−4329.

(14) Popczun, E. J.; Read, C. G.; Roske, C. W.; Lewis, S.; Schaak, R. E. Highly Active Electrocatalysis of the Hydrogen Evolution Reaction by Cobalt Phosphide Nanoparticles. *Angew. Chem., Int. Ed.* **2014**, *53*, 5427−5430.

(15) Faber, M. S.; Dziedzic, R.; Lukowski, M. A.; Kaiser, N. S.; Ding, Q.; Jin, S. High-Performance Electrocatalysis Using Metallic Cobalt Pyrite (CoS_2) Micro- and Nanostructures. *J. Am. Chem. Soc.* **2014**, *136*, 10053−10061.

(16) Gao, M.; Yao, W.; Yao, H.; Yu, S. Synthesis of Unique Ultrathin Lamellar Mesostructured $CoSe_2$−Amine (Protonated) Nanobelts in a Binary Solution. *J. Am. Chem. Soc.* **2009**, *131*, 7486−7487.

(17) Kong, D.; Cha, J. J.; Wang, H.; Lee, H. R.; Cui, Y. First-Row Transition Metal Dichalcogenide Catalysts for Hydrogen Evolution Reaction. *Energy Environ. Sci.* **2013**, *6*, 3553−3558.

(18) Faber, M. S.; Lukowski, M. A.; Ding, Q.; Kaiser, N. S.; Jin, S. Earth-Abundant Cobalt Pyrite (CoS_2) Thin Film on Glass as a Robust, High-Performance Counter Electrode for Quantum Dot-Sensitized Solar Cells. *J. Phys. Chem. C* **2014**, *118*, 21347−21356.

(19) Kong, D.; Wang, H.; Lu, Z.; Cui, Y. $CoSe_2$ Nanoparticles Grown on Carbon Fiber Paper: An Efficient and Stable Electrocatalyst for Hydrogen Evolution Reaction. *J. Am. Chem. Soc.* **2014**, *136*, 4897−4900.

(20) Xu, Y.; Gao, M.; Zheng, Y.; Jiang, J.; Yu, S. Nickel/Nickel(II) Oxide Nanoparticles Anchored onto Cobalt(IV) Diselenide Nanobelts for the Electrochemical Production of Hydrogen. *Angew. Chem., Int. Ed.* **2013**, *52*, 8546−8550.

(21) Gao, M.; Liang, J.; Zheng, Y.; Xu, Y.; Jiang, J.; Gao, Q.; Li, J.; Yu, S. An Efficient Molybdenum Disulfide/Cobalt Diselenide Hybrid Catalyst for Electrochemical Hydrogen Generation. *Nat. Commun.* **2015**, *6*, 5982.

(22) Zhao, W.; Zhang, C.; Geng, F.; Zhuo, S.; Zhang, B. Nanoporous Hollow Transition Metal Chalcogenide Nanosheets Synthesized via the Anion-Exchange Reaction of Metal Hydroxides with Chalcogenide Ions. *ACS Nano* **2014**, *8*, 10909−10919.

(23) Gao, M.; Cao, X.; Gao, Q.; Xu, Y.; Zheng, Y.; Jiang, J.; Yu, S. Nitrogen-Doped Graphene Supported $CoSe_2$ Nanobelt Composite Catalyst for Efficient Water Oxidation. *ACS Nano* **2014**, *8*, 3970−3978.

(24) Xing, Z.; Liu, Q.; Asiri, A. M.; Sun, X. Closely Interconnected Network of Molybdenum Phosphide Nanoparticles: A Highly Efficient Electrocatalyst for Generating Hydrogen from Water. *Adv. Mater.* **2014**, *26*, 5702−5707.

DOI: 10.1021/am509185x
ACS Appl. Mater. Interfaces 2015, 7, 3877−3881

(25) Merki, D.; Hu, X. Recent Developments of Molybdenum and Tungsten Sulfides as Hydrogen Evolution Catalysts. *Energy Environ. Sci.* **2011**, *4*, 3878−3888.
(26) Tian, J.; Liu, Q.; Liang, Y.; Xing, Z.; Asiri, A. M.; Sun, X. FeP Nanoparticles Film Grown on Carbon Cloth: An Ultrahighly Active 3D Hydrogen Evolution Cathode in Both Acidic and Neutral Solutions. *ACS Appl. Mater. Interfaces* **2014**, *6*, 20579−20584.
(27) Kibsgaard, J.; Chen, Z.; Reinecke, B. N.; Jaramillo, T. F. Engineering the Surface Structure of MoS_2 to Preferentially Expose Active Edge Sites for Electrocatalysis. *Nat. Mater.* **2012**, *11*, 963−969.
(28) Roy-Mayhew, J. D.; Boschloo, G.; Hagfeldt, A.; Aksay, I. A. Functionalized Graphene Sheets as a Versatile Replacement for Platinum in Dye-Sensitized Solar Cells. *ACS Appl. Mater. Interfaces* **2012**, *4*, 2794−2800.
(29) Luo, Y.; Jiang, J.; Zhou, W.; Yang, H.; Luo, J.; Qi, X.; Zhang, H.; Denis, Y.; Li, C. M.; Yu, T. Self-assembly of Well-ordered Whisker-like Manganese Oxide Arrays on Carbon Fiber Paper and its Application as Electrode Material for Supercapacitors. *J. Mater. Chem.* **2012**, *22*, 8634−8640.
(30) Guo, C.; Zhang, L.; Miao, J.; Zhang, J.; Li, C. M. DNA-Functionalized Graphene to Guide Growth of Highly Active Pd Nanocrystals as Efficient Electrocatalyst for Direct Formic Acid Fuel Cells. *Adv. Energy Mater.* **2013**, *3*, 167−171.

DOI: 10.1021/am509185x
ACS Appl. Mater. Interfaces 2015, 7, 3877−3881